JOURNAL OF MAGNETIC RESONANCE **131,** 69–85 (1998)
ARTICLE NO. MN971313

Non-Mono-Exponential Attenuation of Water and *N*-Acetyl Aspartate Signals Due to Diffusion in Brain Tissue

Yaniv Assaf and Yoram Cohen[1]

School of Chemistry, The Raymond and Beverly Sackler Faculty of Exact Sciences, Tel Aviv University, Ramat Aviv, Tel Aviv 69978, Israel

Received March 5, 1997; revised October 16, 1997

Diffusion measurements were performed on water and *N*-acetyl aspartate (NAA) molecules in excised brain tissue using a wide range of *b*-values (up to 28.3×10^6 and 35.8×10^6 s cm^{-2} for water and NAA, respectively). The attenuation of the signals of water and NAA due to diffusion was measured at fixed diffusion times (t_D). These measurements, in which the echo time (TE) was set to 70 ms, were repeated for several diffusion times ranging from 35 to 305 ms. Signal attenuations were fitted to mono-, bi-, and triexponential functions to obtain the apparent diffusion coefficients (ADCs) of these molecules at each diffusion time. From these experiments the following observations and conclusions were made: (1) Signal attenuation of water and NAA due to diffusion over the entire range of *b* values examined is not monoexponential and the extracted ADCs depend on the diffusion time; (2) In the case of water the experimental data are best fitted by a triexponential function, while for *b* values up to 1×10^6 s cm^{-2}, a biexponential function seems to reproduce the experimental data as well as the triexponential function; (3) If only the low range of *b* values are fitted (up to 0.5×10^6 s cm^{-2}) signal attenuation of water is monoexponential and insensitive to t_D; (4) Water ADCs decreased with the increase in t_D but the relative population of the fast diffusing component increases such that at a t_D of 305 ms there is nearly a single population; (5) The major fast diffusion component of the water shows only very limited restriction; (6) NAA signal attenuation is biexponential and analysis of the low *b*-value range gives only monoexponential decay, but the obtained ADC is sensitive to the diffusion time; (7) The ADCs obtained from fitting the data with a biexponential function decrease as diffusion time increases; (8) The relative population of the slow-diffusing component decreases with increasing t_D; (9) Both the fast and the slow diffusing components of NAA show a considerable restriction by what seems to be a nonpermeable barrier from which two compartments, one of 7–8 μm and one of $\sim$1 μm, were calculated using the Einstein equation. It is suggested that the two compartments represent the NAA in cell bodies and in the intra-axonal space. The effect of the range of the *b* value used in the diffusion experiments on the results is discussed and used to reconcile some of the apparent discrepancies obtained in different experiments concerning water diffusion in brain tissue. The potential of NAA diffusion experiments to probe cellular structure is discussed.

[1] To whom correspondence should be addressed. Fax: 972-3-6409293. E-mail: ycohen@ccsg.tau.ac.il.

INTRODUCTION

Water diffusion, as deduced from diffusion-weighted MRI (DWI) (*1–3*), is used in the characterization of several neurological disorders (*4–15*). The ability of DWI to discriminate between different pathophysiological states and its high sensitivity to early ischemic events in brain tissue prompted experimental and theoretical studies on water diffusion in biological tissues (*16–27*). Many of these studies were aimed at revealing the cause of the reduction in the ADC after an ischemic event (*8, 9, 16–26*). Cytotoxic edema (*4, 16*), temperature decrease (*17*), changes in membrane permeability (*18*), and increased tortuosity of the extracellular space (*19, 20*) were claimed to be the main contributors to the above observation, suggesting that water diffusion in brain tissue depends, *inter alia*, on the geometry and the structural characteristics of brain tissue.

In principal, the interpretation of NMR signal attenuation due to diffusion in biological tissues is by no means simple. This is due to the fact that NMR diffusion experiments are in fact sensitive to the diffusion path of the diffusing spins (*28*). It is also known that from the diffusion path, or more accurately from the root mean square (rms) displacement, ($\sqrt{\langle x^2 \rangle}$), one can derive the diffusion coefficient using the Einstein equation [1],

$$\sqrt{\langle x^2 \rangle} = \sqrt{2Dt_D} \qquad [1]$$

where $\sqrt{\langle x^2 \rangle}$ is the root mean square path of the investigated molecule during the diffusion time, D is the diffusion coefficient, and t_D is the diffusion time. It should be noted that this equation is applicable only if one assumes a Gaussian distribution, the existence of one population, and no background gradients.

In biological tissues we cannot, *a priori*, assume a Gaussian distribution and thus the Einstein equation may fail (*28*). In such tissues the diffusion of the molecule may be restricted. Consequently the mean displacement may depend on the diffusion time and on the number and type of obstacles

1090-7807/98 $25.00

that prevail in the sample (*28*). Therefore, the term of ''apparent diffusion coefficient'' (ADC) is accepted to describe diffusion in biological systems. In reality, the interpretation of the NMR signal attenuation due to diffusion in biological tissue is even more complex because of the possibility of having more than one population. If the different populations differ in their diffusion coefficients and relaxation times, signal attenuation becomes a function of the diffusion coefficients and of a variety of experimental parameters.

The fact that signal attenuation in NMR diffusion experiments depends on the diffusion path complicates the interpretation of the data on one hand but, on the other hand, provides a mean of studying structural characteristics of the biological sample under investigation. This is extremely important in studying biological samples since NMR diffusion techniques are the only noninvasive techniques which permit the monitoring of diffusion on micrometer scale.

In recent years most diffusion studies of biological tissues in general and of brain tissue in particular have been performed by monitoring water diffusion because of the high signal to noise ratio (SNR) of the water signal in tissue (*1–28*). Indeed, over the last six years only, hundreds of papers have been published dealing with water diffusion in brain, most of which dealt with changes in ADC due to stroke (*3–9, 16–22*). Despite the potential of obtaining tissue microstructure from NMR diffusion experiments, it seems that extracting structural information from water diffusion is difficult, *inter alia*, since water appears in all the compartments and exchanges relatively quickly between them.

One way to obtain additional structural information about brain tissue is to study the diffusion characteristics of intracellular metabolites despite the unfavorable SNR as compared to water. The most suitable candidate for this purpose in the ^{1}H-NMR brain spectrum is the peak at 2.023 ppm attributed to *N*-acetyl aspartate (NAA). NAA has a relatively large and sharp peak in the ^{1}H water-suppressed brain spectrum and its relatively high concentration ($\sim$7–8 mmole (*33, 34*)) gives adequate SNR within a reasonable amount of time. In addition, NAA is present only in the intracellular space of neurons and in the *in vivo* state the cell membrane represents an impermeable barrier for NAA molecules. Nevertheless, only a few studies have been performed on the diffusion of NAA or other metabolites (*35–40*). Most of the studies concerning the diffusion of NAA in brain tissue have been performed using a single diffusion time and by acquiring only a few data points with relatively low *b* values (*36–41*). The effect of the diffusion time on NAA diffusion was reported only in a single study and for monoexponential decay (*42, 43*). Therefore, we decided to concentrate on studying the diffusion characteristics of NAA in the brain and to compare them with those of brain water.

Our NMR diffusion experiments were performed on excised brain tissues using very high *b* values (up to 28.3×10^6 and 35.8×10^6 s cm^{-2} for water and NAA, respectively). We have used a large number of data points from which we observe a nonmonoexponential decay of the signals of both NAA and water. We also examined the changes in the diffusion coefficients as a function of the diffusion time. Our data clearly show that in the low *b* values range, the decay of the water signal is monoexponential and independent of t_D, while analysis of the entire *b* value range shows nonmonoexponential signal attenuation which is dependent on the diffusion time. For NAA the low *b* value range gives a monoexponential decay which depends on t_D while the entire *b* value range could be fitted only by a biexponential function. It was found that NAA shows a more pronounced restricted diffusion than water. Our results imply that diffusion measurements of NAA may give additional information concerning cell size and may serve as a better reporter than water regarding the intracellular milieu and the cell structure.

MATERIALS AND METHODS

Tissue Preparation

Experiments were performed on excised brain tissue taken from Sprague–Dawley rats ($n = 18$) weighting between 120 and 150 g. The rats were euthanized with a bolus of ethyl carbamate (4 g/kg). The brains were washed with deuterated saline to remove blood and blood vessels. The residual deuterated saline served as a lock signal. The brain sample which included the two hemispheres was introduced into a 5 mm NMR tube in a random way with no specific alignment. The removal of the brains and the adjustment of other experimental parameters (shimming and pulses length) took around 20–30 min. The time which elapsed from animal euthanization until the end of the experiment was no longer than 4 h.

NMR Experiments

Diffusion experiments were acquired on an 11.7T narrowbore, ARX spectrometer (Bruker, Karlsruhe, Germany) using a commercial 5-mm inverse probe equipped with a set of self-shielded, *z*-gradient coils. Gradient pulses were generated using a B-AFPA 10 linear amplifier and a BGU unit was used for preemphasis.

Water diffusion experiments ($n = 3$) were obtained using the stimulated echo diffusion sequence (*29*). Echo selection was achieved by the conventional phase cycling program,

$$\pi/2-\tau_1-g-\tau_2-\pi/2-T_M-\pi/2-\tau_2-g-\tau_1-Acq. \quad [I]$$

In our experiments τ_1 and τ_2 were set to 10 ms to avoid any residual eddy currents even at high gradient strength and the duration of the pulsed gradient (g) was set to 15 ms, resulting

in a TE of 70 ms. The pulsed gradient strength was incremented from 0 to 24 gauss cm^{-1} (24 gradient steps) for each T_M value which was varied between 5 and 275 ms giving a diffusion time (t_D) between 35 and 305 ms. The maximal b values in these experiments were 3.2×10^6 and 28.3×10^6 s cm^{-2} for the diffusion times of 35 and 305 ms, respectively. In the brain water experiments a capillary of *tert*-butanol was inserted to verify spectrometer and gradient stability.

We also examined the effect of background gradients (g_0). In the presence of background gradients, the signal attenuation due to diffusion depends on three general terms, namely g^2, gg_0, and g_0^2. The gg_0 term can cause significant miscalculations of the b value, but by adding two sets of diffusion experiments, in which the diffusion sensitizing pulse gradients (g) are given in opposite polarity, it is possible to cancel the effect of gg_0 (44). Therefore, we performed a set of such experiments in order to estimate the influence, if any, of background gradients on our measurements. In addition, the values of T_2 and T_1 ($n = 3$) were measured for water using the CPMG and the inversion recovery pulse sequences, respectively. T_1 relaxation times were extracted from fully relaxed spectra obtained with a repetition time (TR) of 30 s. For the T_2 measurements TR was set to 5 s (and four dummy scans were used to achieve steady state).

NAA diffusion experiments ($n = 3$) were also collected using the stimulated echo diffusion sequence (*29*) with water suppression (a 100 ms low power pulse on the water frequency). In these experiments τ_1, τ_2, and T_M had the same values as specified above. The pulsed gradients duration was 15 ms and their strength was incremented between 0 and 27 gauss cm^{-1} (in 14 steps). T_M was incremented between 5 and 275 ms, resulting in diffusion times of 35 and 305 ms, respectively. The maximal b values in these experiments were 4.1×10^6 and 35.8×10^6 s cm^{-2} for the diffusion times of 35 and 305 ms, respectively.

The effect of background gradients on the diffusion of NAA was evaluated as described above (*44*) and the T_2 and T_1 ($n = 3$) of NAA were measured using the CPMG and inversion recovery sequences, respectively, with water suppression. Here again TR was set to 30 s for the T_1 measurements and to 5 s for the T_2 experiments (with four dummy scans).

We also examined the effect of the TE on the ADCs of brain water and NAA. The TE should have no effect on the ADC in the absence of background gradients and assuming that there is only one population. In these experiments τ_1 was varied between 10 and 75 ms, resulting in TEs between 70 and 200 ms. This experiments were measured using two values of T_M, 5 and 95 ms, resulting in diffusion times of 35 and 125 ms, respectively.

Since we were studying brain tissue *in vitro*, the changes of the water and the NAA diffusion characteristics during the experiments were evaluated to ensure that the measured parameters did not change drastically throughout. Therefore, we acquired the same diffusion experiments over 3.5 h by keeping all parameters constant (TE was 70 ms, T_M was 5 ms, and diffusion time was 35 ms). Indeed, the measured parameters changed insignificantly throughout the duration of the experiment (see result section). Nevertheless, to avoid systematic errors due to tissue disintegration, experiments with short and long T_M values were collected randomly for both water and NAA. In all diffusion experiments the recovery time was 3 s and the temperature in all NMR experiments was 298 ± 0.1 K.

Since *tert*-butanol has a larger diffusion coefficient than that of the slow component of the NAA, we also measured, in separate experiments, the effect of the diffusion time on oil diffusion in order to verify the stability of our measurements of the slow-diffusing component while using the entire b value range used in the NAA diffusion experiments.

ADC Calculation

ADCs were calculated by fitting the attenuation of the experimental signal to the expression

$$I/I_0 = \sum_n A_n \exp[-\gamma^2\delta^2 g^2(\Delta - \delta/3)D_n] = \sum_n A_n \exp(-bD_n) \quad [2]$$

where I and I_0 are the signal intensities in the presence and absence of diffusion sensitizing gradients, A_n is the relative weighting of each fitted population, γ is the gyromagnetic ratio, g is the pulsed gradient strength, δ is the pulsed gradient duration, $\Delta - \delta/3$ is the effective diffusion time, and D_n is the apparent diffusion coefficient of each fitted population. The data were fitted using the LM (Levenberg–Marquardt) nonlinear least-squares routine provided by Microcal Origin (Microcal Software Inc., Northampton, MA). The attenuation of the *tert*-butanol and the oil signals was perfectly fitted by a monoexponential decay, while the signal attenuations of water and NAA were fitted to mono-, bi-, and triexponential decays. The NAA signal attenuation was best fitted to a biexponential decay and the water signal attenuation was best fitted by a triexponential decay function.

The intensity of the water and NAA peaks was obtained from the phase sensitive signals by evaluating their intensity using an automated peak height determination procedure. Generally, no significant line broadening was observed. In a few cases only, at high b-values, we observed a saddle line broadening at the shortest diffusion time.

The T_1 and T_2 data for both water and NAA were also fitted to mono-, bi-, and triexponential decays. Only the values of the best fit in each case are reported.

RESULTS

Diffusion Characteristics of Brain Water

Diffusion experiments on brain water were all carried out in the presence of a capillary of *tert*-butanol as an external standard. As expected, the signal attenuation of the *tert*-butanol gave a monoexponential decay and a plot of $\ln(I/I_0)$ against the entire b value range gave a straight line ($r^2 \geq 0.9999$) from which a diffusion coefficient of $0.309(\pm 0.003) \times 10^{-5}$ cm^{2}s^{-1} was calculated. This value is in good agreement with the value reported in the literature (*40*) and was found to be, as expected, insensitive to the diffusion time. A plot of $\ln(I/I_0)$ as a function of b values for the oil, which is characterized by slow diffusion, also gave a straight line ($r^2 \geq 0.999$) which was insensitive to the diffusion time. We have calculated a self-diffusion coefficient of $0.030(\pm 0.003) \times 10^{-5}$ cm^{2}s^{-1} for the oil. These experiments were aimed to test gradient stability up to the highest b value used in the current study.

Although a plot of $\ln(I/I_0)$ against b values of *tert*-butanol and oil gave straight lines, the very same plot for brain water deviated considerably from linearity suggesting a multi-exponential decay. Interestingly, the dependency of $\ln(I/I_0)$ on the b values for brain water changes with the diffusion time ($\Delta - \delta/3$), although no such dependency has been observed for the *tert*-butanol and oil signals as shown in Fig. 1A. It is important to note that the deviation of $\ln(I/I_0)$ of brain water from linearity is not apparent for b values smaller than 0.5×10^6 s cm^{-2}. This deviation from linearity observed at high b values is larger for shorter diffusion times than that observed for longer diffusion times (Fig. 1). Fig. 1B is a zoom of the data presented in Fig. 1A for b values in the range from 0 to 1×10^6 s cm^{-2}. The zooming of the data clearly demonstrates that the dependency of the results on the diffusion time is not apparent over this range of b values. Figure 2 shows the fit of the experimental data, obtained at diffusion times of 35 and 305 ms, to mono-, bi-, and triexponential decay functions according to Eq. [2]. It is clear that the monoexponential decay fails to reproduce the experimental data and that there is already much better agreement between the experimental data and the biexponential decay fit. However, the triexponential decay fit gives further improvement in the agreement between the experimental and the fitted data as compared to the biexponential fit. Interestingly, based on *in vivo* and *in vitro* ^{2}H double quantum filter NMR spectroscopy, the existence of at least three water populations was suggested (*45, 46*).

Figures 3A and 3B show the changes in the ADCs of brain water obtained by the bi- and triexponential fits as a function of the diffusion times and the calculated diffusion coefficient of *tert*-butanol. Figures 4A and 4B show the changes in the relative fraction of each of the fitted water

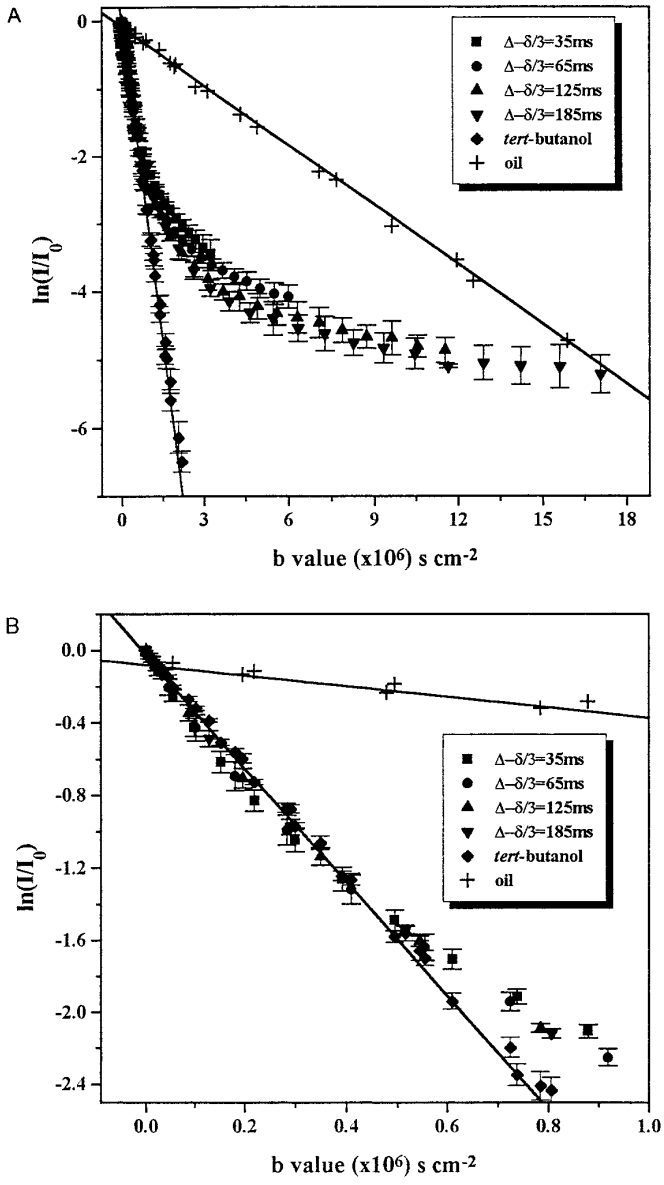

FIG. 1. Normalized signal attenuation ($\ln(I/I_0)$) of *tert*-butanol, oil, and brain water signals ($n = 3$) for four different diffusion times ($\Delta - \delta/3$) as a function of the b value. (A) b values up to 18×10^6 s cm^{-2} and (B) same data for b values up to 1×10^6 s cm^{-2}. The data show that the attenuation of the signal intensity of the *tert*-butanol and oil are monoexponential and are insensitive to the diffusion time, while that of brain water is not monoexponential and depend on the diffusion time. The data for the different four diffusion times of *tert*-butanol are all superimposed. The deviation from linearity decreases as the diffusion time increases. Interestingly, the zooming of the data shown in (B) demonstrates that for b-values up to 1×10^6 s cm^{-2} the results are insensitive to the diffusion time. These graphs show that up to b values of $0.4–0.5 \times 10^6$ s cm^{-2} the decay is nearly monoexponential.

populations as a function of the diffusion times for the bi- and triexponential fitting, respectively. Table 1 depicts the apparent diffusion coefficients (ADCs) and the relative pop-

ulations as a function of the diffusion times as obtained from fitting the experimental data to mono-, bi-, and triexponential functions according to Eq. [2]. From Table 1 and Figs. 3 and 4 one can see that the extracted ADCs decrease with increased diffusion time. This decrease is accompanied by changes in the relative populations of each component. However, close inspection of the data in Table 1 reveals the following additional results: (1) Data fit in the low b values range ($b \leq 5 \times 10^5$ s cm^{-2}), usually used in diffusion weighted MRI, results in a single ADC of $0.26(\pm 0.02) \times 10^{-5}$ cm^{2}s^{-1}, a value which was found to be insensitive to the diffusion time. (2) The ADCs obtained from biexponential fitting were found to be sensitive to the diffusion time. The ADC of the fast diffusing component decreases from $0.44(\pm 0.01) \times 10^{-5}$ to $0.27(\pm 0.01) \times 10^{-5}$ cm^{2}s^{-1} when the diffusion time increases from 35 to 305 ms, and its relative fraction increases from 83(±1) to 98(±1)%. The slow component shows a more dramatic decrease in its ADC, from $0.058(\pm 0.003) \times 10^{-5}$ to $0.008(\pm 0.001) \times 10^{-5}$ cm^{2}s^{-1}, and its fraction decreases from 17(±1) to 2(±1)% when the diffusion time increases from 35 to 305 ms. These results imply that at a diffusion time of 305 ms only one

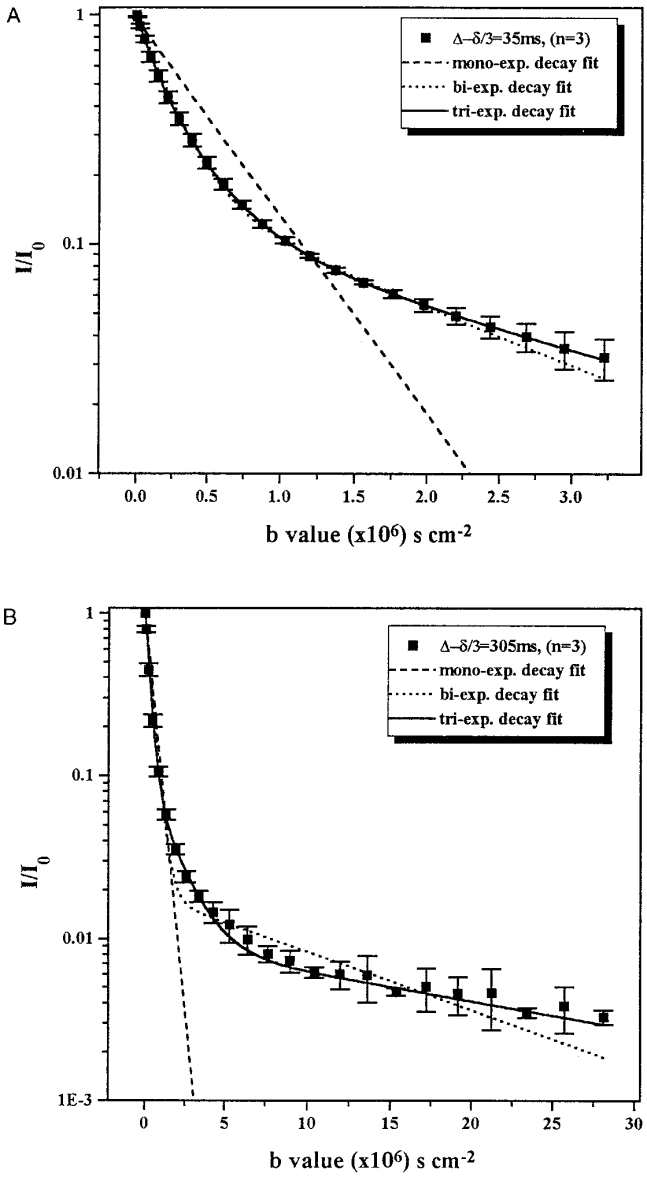

FIG. 2. Normalized signal attenuation (I/I_0) (on a logarithmic scale) of brain water signal ($n = 3$) as a function of the b value along with the mono-, bi-, and triexponential fits for (A) the shortest (35 ms) and (B) the longest (305 ms) diffusion times used in the diffusion experiments. The graphs clearly indicate that the triexponential decay function reproduces the experimental data better than the bi- and monoexponential fits; the monoexponential fit is the worst.

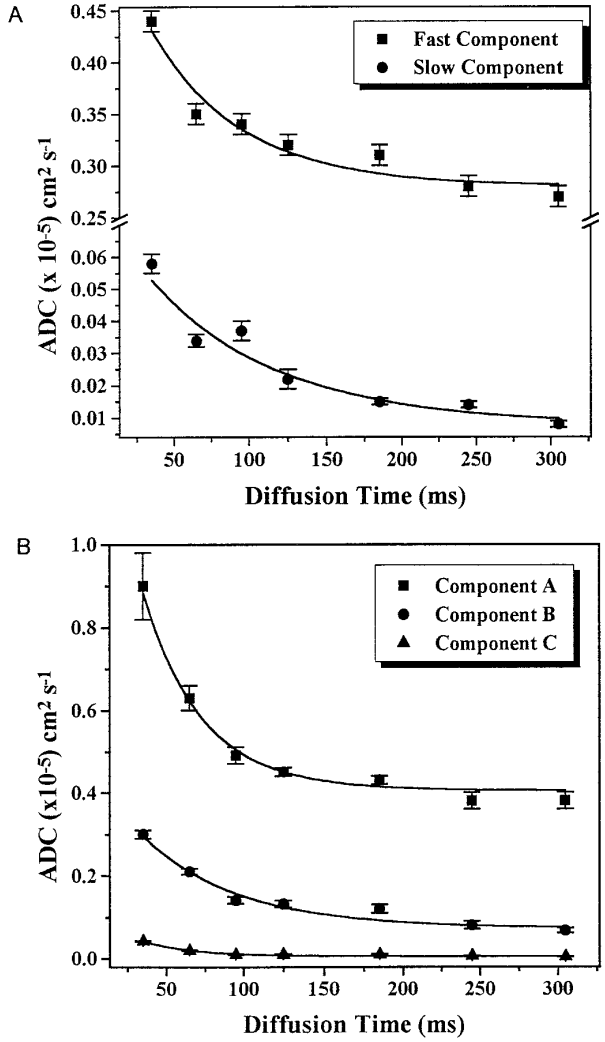

FIG. 3. The ADCs ($n = 3$) obtained from the (A) biexponential and (B) triexponential fitting functions as a function of the diffusion time. These graphs clearly demonstrate that the ADCs decrease with the increase in diffusion time. The solid lines are arbitrary and are used just to guide the eye.

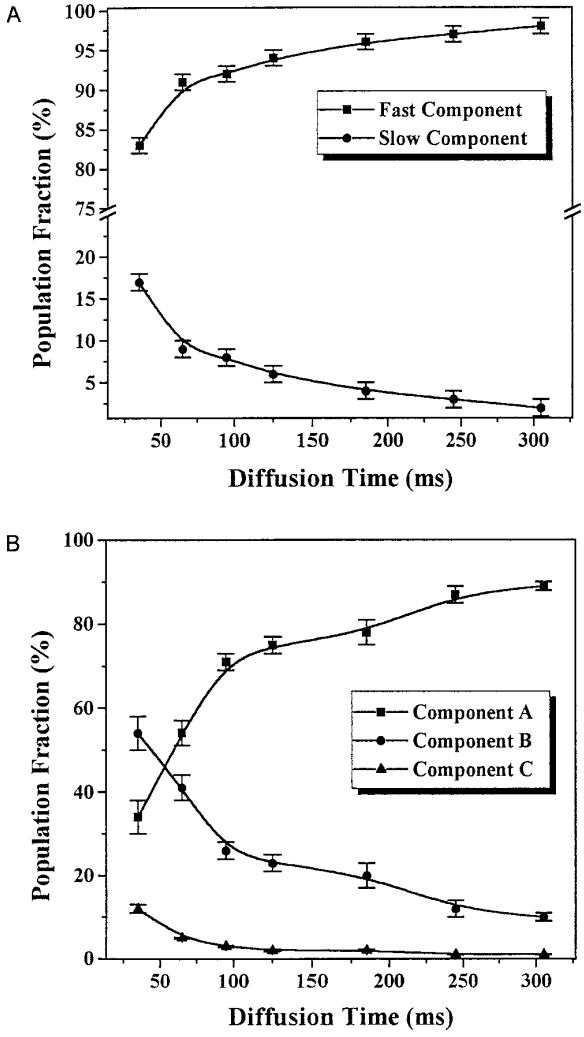

FIG. 4. The changes in the relative population of each of the ADCs ($n = 3$) as a function of the diffusion time: (A) ADC populations obtained from the biexponential fit and (B) ADC populations obtained from the triexponential fit. Here it is clear that the diffusion time has a dramatic effect on the relative population of each ADC. The solid line are arbitrary and are used just to guide the eye.

component prevails in practice. (3) The ADCs obtained from the triexponential fitting were also found to be sensitive to the diffusion time. In this case the fast diffusion component of the water first shows a fast decline in its ADC from $0.90(\pm0.08) \times 10^{-5}$ to $0.45(\pm0.01) \times 10^{-5}$ cm^2s^{-1} while its relative population increases from $34(\pm4)$ to $75(\pm2)$% when the diffusion time is increased from 35 to 125 ms. At the longer diffusion times the ADC of the fast diffusing component declines slowly from $0.45(\pm0.01) \times 10^{-5}$ cm^2s^{-1} at diffusion time of 125 ms to $0.38(\pm0.01) \times 10^{-5}$ cm^2s^{-1} at diffusion time of 305 ms while its relative fraction increased to $89(\pm1)$% at a diffusion time of 305 ms. In contrast to the fast diffusing component, the ADC of the intermediate component decreases more monotonically from $0.30(\pm0.01) \times 10^{-5}$ cm^2s^{-1} at a diffusion time of 35 ms to $0.068(\pm0.006) \times 10^{-5}$ cm^2s^{-1} at a diffusion time of 305 ms while its relative population decreases from $54(\pm4)$ to $10(\pm1)$%. The slow diffusing component shows a similar trend as its ADC drops gradually from $0.042(\pm0.001) \times 10^{-5}$ cm^2s^{-1} at a diffusion time of 35 ms to $0.004(\pm0.0004) \times 10^{-5}$ cm^2s^{-1} at a diffusion time of 305 ms, while its relative population decreases from $12(\pm4)$ to $1(\pm0.1)$%. When the diffusion time is 305 ms it seems that the dominant population is the one that has the highest ADC.

To test for the existence of restricted diffusion we plotted the diffusion distance as calculated by the Einstein equation (Eq. [1]) versus the square root of the diffusion time as shown in Figs. 5A and 5B. In Fig. 5A, which depict the data obtained from the biexponential fitting, although a clear restriction is observed for the slow diffusing components only a very limited restriction, if any, is observed for the large fast diffusing component. The *tert*-butanol, however, shows no restriction, as shown by the straight line that can be drawn between the experimental points and the origins. The data in Fig. 5B, deduced from the triexponential fit, demonstrate that there is some deviation from linearity in the dependency of the mean diffusion path on the square root of the diffusion time even for the fast diffusing component. The other two components show a much more significant deviation from linearity, indicating a much more pronounced restriction.

Because we are dealing with an *in vitro* sample, we had to examine the changes in the measured parameters over the experimental time to assess changes due to sample disintegration. This was done by repeating the same experiment over 3.5 h. It was found that the ADC of the fast diffusing component increases at a rate of 0.005×10^{-5} cm^2s^{-1} per hour while the intermediate and slow diffusion coefficients decrease at rates of 0.002×10^{-5} and 0.003×10^{-5} cm^2s^{-1} per hour, respectively. The changes of the population fractions over the duration of the experiment were found to be much smaller than those observed when the diffusion time was changed. The fraction of the fast diffusing population increased by 3.5% per hour while the intermediate and slow populations decreased by 2.5% per hour and 1% per hour, respectively. It should be noted that the changes observed for the ADC of the fast diffusing component actually show the opposite trend as compared to the changes observed with the increase in the diffusion time.

Since several populations were observed in the diffusion experiments we have also measured the T_1 and T_2 of the brain water. The T_1 was found to have a monoexponential decay from which a value of $2.1(\pm0.1)$s ($n = 3$) was calculated. The T_2 was found to be biexponential and the two values obtained were a T_2 (fast) of $11(\pm9)$ ms with a relative population of $20(\pm9)$% and a T_2 (slow) of $46(\pm7)$ ms

TABLE 1

The Effect of the Diffusion Time (Δ-δ/3) on the Diffusion Coefficients of *tert*-Butanol and Oil and on the ADC of Brain Water as Obtained by Fitting the Experimental Data to Mono-,[a] Bi-, and Triexponential Decay Functions

		Brain water							
Δ-δ/3 (ms)	fit	D_1 ($\times 10^{-5}$) cm^2 s^{-1}	A_1 (%)	D_2 ($\times 10^{-5}$) cm^2 s^{-1}	A_2 (%)	D_3 ($\times 10^{-5}$) cm^2 s^{-1}	A_3 (%)	*tert*-Butanol D ($\times 10^{-5}$) cm^2 s^{-1}	Oil D ($\times 10^{-5}$) cm^2 s^{-1}
35	mono	0.27 ± 0.01	—	—	—	—	—	0.312 ± 0.001	0.033
	bi	0.44 ± 0.01	83 ± 1	0.058 ± 0.003	17 ± 1	—	—	—	—
	tri	0.90 ± 0.08	34 ± 4	0.30 ± 0.01	54 ± 4	0.042 ± 0.001	12 ± 4	—	—
65	mono	0.27 ± 0.01	—	—	—	—	—	0.301 ± 0.001	—
	bi	0.35 ± 0.01	91 ± 1	0.034 ± 0.002	9 ± 1	—	—	—	—
	tri	0.63 ± 0.03	54 ± 3	0.210 ± 0.007	41 ± 3	0.020 ± 0.001	5.0 ± 0.2	—	—
95	mono	0.26 ± 0.01	—	—	—	—	—	0.304 ± 0.001	—
	bi	0.34 ± 0.01	92 ± 1	0.037 ± 0.003	8 ± 1	—	—	—	—
	tri	0.49 ± 0.02	71 ± 2	0.141 ± 0.008	26 ± 2	0.010 ± 0.001	3.0 ± 0.2	—	—
125	mono	0.27 ± 0.01	—	—	—	—	—	0.303 ± 0.001	0.028
	bi	0.32 ± 0.01	94 ± 1	0.022 ± 0.003	6 ± 1	—	—	—	—
	tri	0.45 ± 0.01	75 ± 2	0.132 ± 0.008	23 ± 2	0.010 ± 0.001	2.0 ± 0.2	—	—
185	mono	0.27 ± 0.02	—	—	—	—	—	0.301 ± 0.001	—
	bi	0.31 ± 0.01	96 ± 1	0.015 ± 0.001	4 ± 1	—	—	—	—
	tri	0.43 ± 0.01	78 ± 3	0.12 ± 0.01	20 ± 3	0.010 ± 0.001	2.0 ± 0.2	—	—
245	mono	0.28 ± 0.02	—	—	—	—	—	0.300 ± 0.001	—
	bi	0.28 ± 0.01	97 ± 1	0.014 ± 0.001	3 ± 1	—	—	—	—
	tri	0.38 ± 0.02	87 ± 2	0.081 ± 0.009	12 ± 2	0.006 ± 0.001	1.0 ± 0.1	—	—
305	mono	0.26 ± 0.02	—	—	—	—	—	0.300 ± 0.001	0.030
	bi	0.27 ± 0.01	98 ± 1	0.008 ± 0.001	2 ± 1	—	—	—	—
	tri	0.38 ± 0.02	89 ± 1	0.068 ± 0.006	10 ± 1	0.0041 ± 0.0004	1.0 ± 0.1	—	—

[a] Linear region up to b values of 0.5×10^{-6} s cm^{-2}.

having a relative population of 80(±9)% (see Table 2). Changing the TE had no effect on the results obtained from the diffusion experiments as can be seen from the data in Table 3. Experiments performed to assess the relative contribution of background gradients show that background gradients are, as expected, relatively unimportant (data not shown).

Diffusion Characteristics of N-Acetyl Aspartate in Brain Tissue

Like the diffusion of brain water, the NAA diffusion shows a multiexponential behavior which could be fitted by a biexponential function. Figure 6 shows three series of spectra of NAA diffusion experiments at three different diffusion times (35, 125, and 305 ms) in which the pulsed gradient strength was adjusted so that the resulting b values would be the same in each of the increments of the three series of spectra. The fact that the signal attenuation in these three stackplots is different suggests that the ADCs do depend on the diffusion time. Figure 7A shows the plot of $\ln(I/I_0)$ as a function of b values ($n = 3$) for three diffusion times (35, 65, and 125 ms) and demonstrates that the signal attenuation is multiexponential and depends on the diffusion time. Interestingly, in the NAA case the deviation from linearity seems to increase as the diffusion time increases. This trend is opposite the trend observed for brain water, but follows the trend recently reported for water in isolated optic nerve (*32*). Analysis of the attenuation of $\ln(I/I_0)$ for b values in the range from 0 to 0.5×10^6 cm^{2}s^{-1} (Fig. 7B) affords straight lines indicative of monoexponential decay. Interestingly, when we analyze only the low b value range, the extracted ADC of NAA is only slightly lower than those reported recently for the *in vivo* state (*41*). This is to be expected since our diffusion experiments were performed at 25°C, a temperature which is lower than that of the *in vivo* state. However, the ADC values obtained from the signal attenuation in this b values range do depend on the diffusion time. Figures 8A and 8B show the decay of I/I_0 (on a logarithmic scale) as a function of the b value for t_D values of 35 and 305 ms along with a mono- and a biexponential fit clearly showing that the entire data set cannot be fitted by a monoexponential function. Table 4 depicts the changes in the ADCs and their relative populations as obtained from the mono- and biexponential fits as a function of the diffusion time. The monoexponential fit was calculated using a low b value range ($b \leq 0.5 \times 10^6$ s cm^{-2}). Figures 9A and 9B are

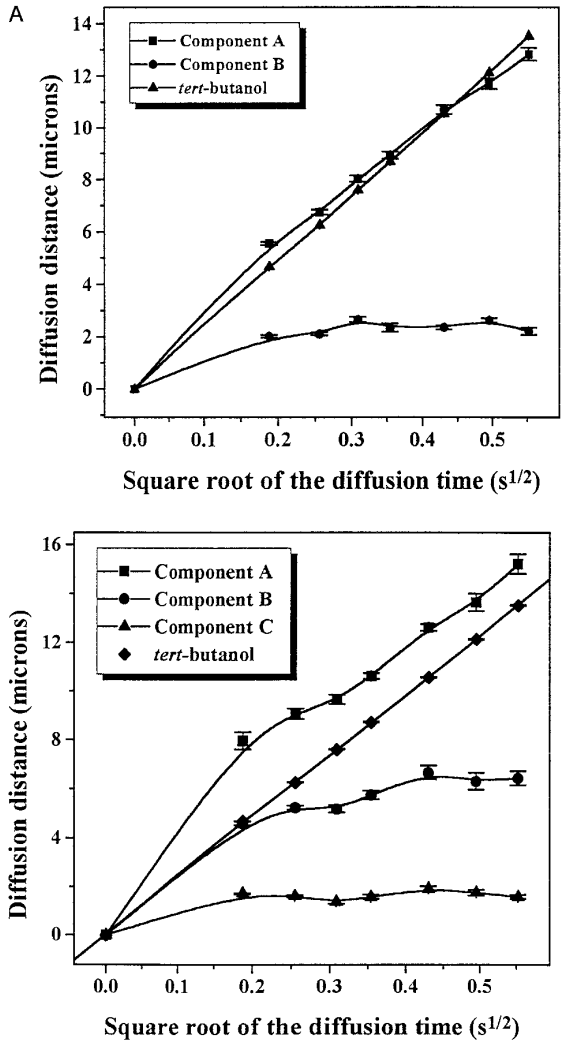

FIG. 5. The ''restriction test'' for different diffusing components of brain water ($n = 3$) as obtained by (A) biexponential fit and (B) triexponential fit, along with that of *tert*-butanol. The plot of the diffusion distance as a function of the square root of the diffusion time ($\sqrt{t_D}$) should give a straight line that passes through the origin if no restriction occurs. The lack of any restriction is apparent for the *tert*-butanol, as expected. From these graphs it is clear that the fast diffusing component of brain water also exhibits only very limited restriction. Beside the *tert*-butanol lines all other lines are arbitrary lines used just to guide the eye.

graphical representations of the drastic changes in the NAA ADCs and their relative fractions (populations) as a function of the diffusion time. The ADC of the fast diffusing component of the NAA decreases from $0.31(\pm0.03) \times 10^{-5}$ cm^2s^{-1} at a diffusion time of 35 ms to $0.077(\pm0.008) \times 10^{-5}$ cm^2s^{-1} at a diffusion time of 305 ms, a fourfold reduction. The slow diffusion component decreases from $0.027(\pm0.001) \times 10^{-5}$ cm^2s^{-1} at a diffusion time of 35 ms to $0.002(\pm0.0002) \times 10^{-5}$ cm^2s^{-1} at a diffusion time of 305 ms, a reduction by a factor of 15. These data also show that the fast diffusing component increases from a relative population of $24(\pm2)$ to $53(\pm1)$%, while its slow component decreases from $76(\pm2)$ to $47(\pm1)$%. The ADC of the slow diffusing component of NAA at long diffusion times is close to the limit of the measurement capability of our system; therefore the relative error in these values is relatively high.

As stated in the case of water, a plot of the diffusion distance versus the square root of the diffusion time may suggest the existence of restricted diffusion. From such a plot for NAA (Fig. 10), it is clear that both the slow and the fast diffusing components are highly restricted. The diffusion distance of the slow diffusing component seems to reach an asymptotic value at relatively short diffusion times.

The changes in NAA diffusion characteristics due to tissue disintegration was studied over a period of four hours. In this experiment we found that the ADC of the fast diffusing component increases at a rate of 0.008×10^{-5} cm^2s^{-1} per hour while its population increases at a rate of 0.8% per hour. The slow component was practically constant and shows a very minor decrease in its ADC of 0.002×10^{-5} cm^2s^{-1} per hour while its population decreased at a rate of 0.8% per hour. This means that the changes in the ADCs and the relative populations of the two components are much smaller than those observed at different diffusion times.

As different NAA components are observed in the diffusion experiments, the relaxation times of the NAA peaks were studied. This was done in order to estimate the effect of T_1, if any, on the diffusion measurements and in order, at a second stage, to try to correlate diffusion and relaxation effects. Since we studied the diffusion characteristics of our sample as a function of the diffusion time by changing the T_M values of the stimulated echo sequence, we have measured the T_1 to verify if by changing the T_M from 35 to 305 ms one has to correct the relative fraction for T_1 effect. In the relaxation time experiments of the NAA peaks, we have found two T_1 populations while the T_2 of the NAA peak revealed three components as depicted in Table 2. The T_1 (fast) was found to be $0.41(\pm0.01)$ s ($n = 3$) with a relative fractional population of $28(\pm4)$% while the T_1 (slow) was found to be $1.42(\pm0.06)$ s with a relative population of $72(\pm4)$%. The T_2 decay of the NAA peak gave three popu-

TABLE 2
Relaxation Times of Brain Water and NAA at 25°C

		Water ($n = 3$)		NAA ($n = 3$)
T_1		2.1 ± 0.1 s	fast	0.41 ± 0.01 s (28 ± 4%)
			slow	1.42 ± 0.06 s (72 ± 4%)
T_2	fast	11 ± 9 ms (20 ± 9%)	fast	19 ± 3 ms (27 ± 3%)
	slow	46 ± 7 ms (80 ± 9%)	int.	241 ± 24 ms (40 ± 5%)
			slow	686 ± 56 ms (33 ± 3%)

TABLE 3
TE Effect of Water and NAA ADCs

	Water[a,b]			NAA[a,b]	
TE (ms)	D_1 ($\times 10^{-5}$) $cm^2\ s^{-1}$	D_2 ($\times 10^{-5}$) $cm^2\ s^{-1}$	D_3 ($\times 10^{-5}$) $cm^2\ s^{-1}$	D_1 ($\times 10^{-5}$) $cm^2\ s^{-1}$	D_2 ($\times 10^{-5}$) $cm^2\ s^{-1}$
70	1.4 (19%)	0.34 (65%)	0.045 (16%)	0.22 (35%)	0.015 (65%)
120	1.8 (18%)	0.34 (65%)	0.048 (16%)	0.41 (20%)	0.020 (80%)
150	—	—	—	0.45 (15%)	0.021 (85%)
200	—	—	—	0.50 (11%)	0.026 (89%)

[a] The diffusion time (Δ-δ/3) in these experiments was set to 35 ms.
[b] Experiments performed with diffusion time 95 ms gave the same effect (data not shown).

lations having T_2 of 19($\pm$3) ms (27 $\pm$ 3%), 241($\pm$24) ms (40 $\pm$ 5%) and 686($\pm$56) ms (33 $\pm$ 3%) (Fig. 11). The effect of the TE on the results obtained from the diffusion experiments for the NAA peak is reported in Table 3. These data clearly demonstrate that in longer TEs the relative populations of the slow diffusing component increases indicating that the slow diffusing component have a longer TE than the fast diffusing component. The effect of TE on the diffusion characteristics of NAA was evaluated for t_D of 35 ms (Table 3) and 95 ms (data not shown). The same effect of TE was seen in the two sets of experiments.

DISCUSSION

Diffusion Characteristics of Brain Water

The results demonstrate that the attenuation of the signal of brain water due to diffusion is not monoexponential and that this multiexponential decay depends on the diffusion time. Most of the diffusion MRS and MRI studies performed on *in vivo* brain water in recent years showed only monoexponential decay of the brain water signal due to diffusion (*3–10*). However, several studies performed using short diffusion times (*21, 22, 31*) and a recent publication, published during the preparation of this manuscript, clearly showed a biexponential decay of water signal due to diffusion in *in vivo* brain and in several pathologies (*47*). In the aforementioned study, the experiments were performed using relatively high *b* values (up to 1×10^6 s cm^{-2}) on several experimental models *in vivo* and most experiments were performed using a single diffusion time. Interestingly, in this recent study when the diffusion time was varied no effect was observed (*47*) although the theoretical model that they have used (*48*) does predict that the diffusion time should have an effect on the results. Some studies on the effect of the diffusion time on the ADC of animal brains have come to the conclusion that the diffusion time has no

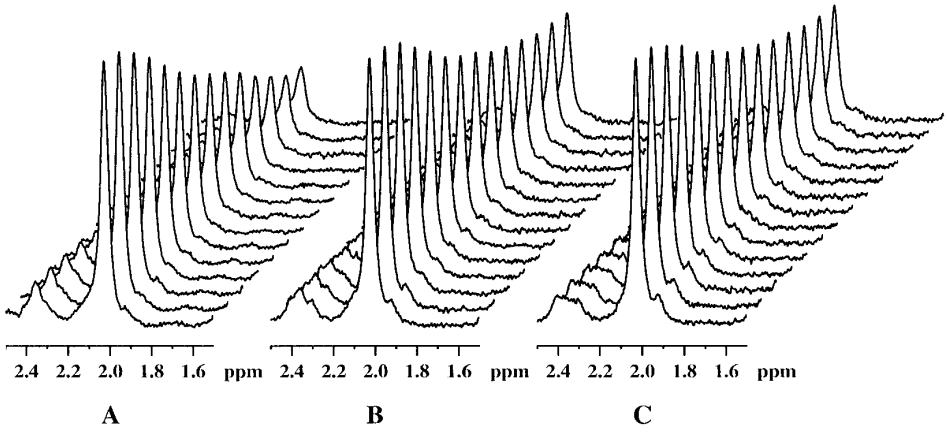

FIG. 6. Attenuation of the signal of NAA as a function of *b* value for three diffusion times. The increments of the pulsed gradient strength were adjusted in the three experiments in order to obtain equal *b* values for each row of the three experiments. The different attenuation profiles obtained, despite the fact that the same *b* values were used in the different experiments suggests that different ADCs are likely to be obtained in each experiment which may indicate the presence of restricted diffusion.

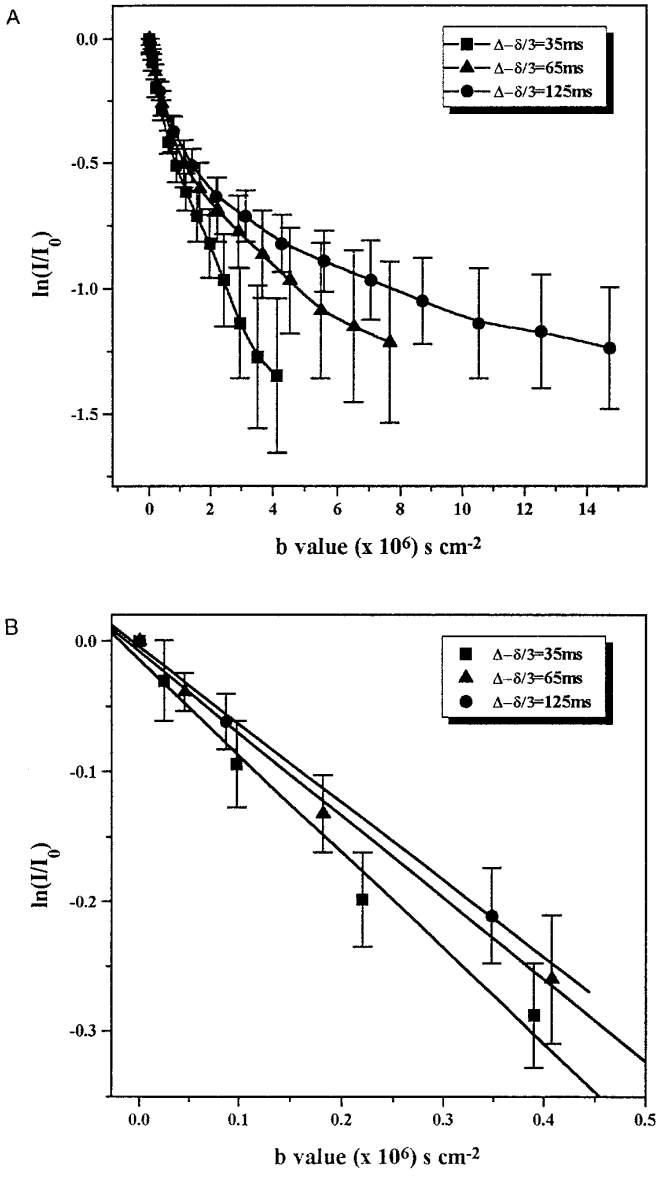

FIG. 7. Normalized signal attenuation ($\ln(I/I_0)$) of NAA in brain tissue ($n = 3$) for three different diffusion times ($\Delta - \delta/3$) as a function of the b value: (A) b values up to 18×10^6 s cm^{-2} and (B) the same data for b values up to 0.5×10^6 s cm^{-2}. The data show that the decay is not monoexponential and depends on the diffusion time. The deviation from linearity increases with the increase in diffusion time. This trend is in fact opposite to that observed for brain water (see Fig. 1) but concurs with the recent report concerning water in isolated excised optic nerve (*32*). The data in the lower b value range support monoexponential decay. However, in these cases the ADC do depend on the diffusion time. The longer the t_D the smaller is the obtained ADC (numerical data are reported in Table 4).

effect whatsoever on the brains ADC (*30*). Yet, the Leibfritz group provided evidence for some restriction of water in *in vivo* brains (*21, 22, 31*) and in brain cells (*49*) while other reported such restriction in nerves (*32*). It seems, therefore, that there is a discrepancy between the different studies reported by the different groups. However, we feel that many of these discrepancies are only apparent and result from the slight differences in the systems studied, but more importantly, from the different parameters used in the different studies. The brain is a complex system and, as explained in the Introduction, the attenuation of the NMR signal due to diffusion is not proportional to the diffusion coefficient but rather to the mean diffusion path. Therefore it is reasonable that in brain tissue, which can be classified as a milieu of restricted geometry, parameters such as the diffusion time or b values should have an effect on the measured apparent diffusion coefficient (ADC).

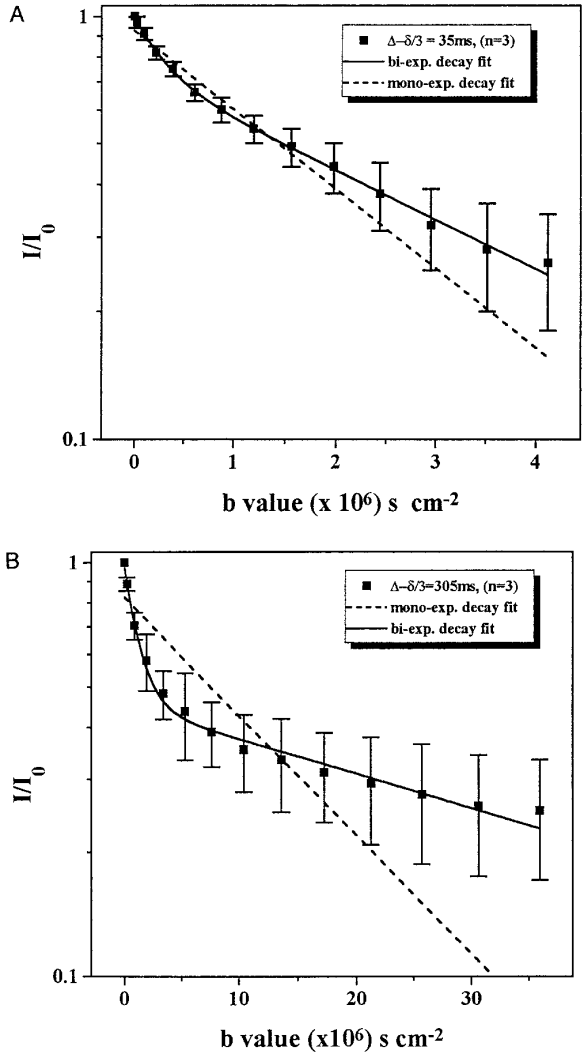

FIG. 8. Normalized NAA signal attenuation ($n = 3$) (on a logarithmic scale) as a function of b value along with the mono- and biexponential fits of the experimental data for (A) the shortest (35 ms) and (B) the longest (305 ms) diffusion times used in our diffusion experiments. The data demonstrate that a much better fit of the experimental data is obtained by the biexponential fitting function.

TABLE 4
The Effect of the Diffusion Time (Δ-δ/3) on the ADC of NAA as Obtained by Fitting the Experimental Data to Mono-[a] and Biexponential Decay Functions

Δ-δ/3 (ms)	fit	D_1 ($\times 10^{-5}$) cm^2 s^{-1}	A_1 (%)	D_2 ($\times 10^{-5}$) cm^2 s^{-1}	A_2 (%)
35	mono	0.089 ± 0.003	—	—	—
	bi	0.31 ± 0.03	24 ± 2	0.027 ± 0.001	76 ± 2
65	mono	0.072 ± 0.004	—	—	—
	bi	0.19 ± 0.01	37 ± 1	0.011 ± 0.001	63 ± 1
95	mono	0.086 ± 0.003	—	—	—
	bi	0.17 ± 0.01	40 ± 1	0.0076 ± 0.0003	60 ± 1
125	mono	0.060 ± 0.003	—	—	—
	bi	0.13 ± 0.01	44 ± 1	0.0050 ± 0.0004	56 ± 1
185	mono	0.048 ± 0.003	—	—	—
	bi	0.110 ± 0.008	45 ± 1	0.0031 ± 0.0002	55 ± 1
245	mono	0.043 ± 0.002	—	—	—
	bi	0.105 ± 0.006	46 ± 1	0.0023 ± 0.0002	54 ± 1
305	mono	0.040 ± 0.002	—	—	—
	bi	0.077 ± 0.008	53 ± 1	0.0019 ± 0.0002	47 ± 1

[a] Linear region up to b values of 0.5×10^{-6} s cm^{-2}.

In order to discuss these apparent discrepancies one has to look at the results in more detail and analyze them by taking into consideration the parameters with which they were obtained. To exemplify this point we report here the result obtained from our data using the different ranges of b values (see Table 1 and Figs. 1A and 1B). If we take into consideration experimental points obtained for b values up to $0.4–0.5 \times 10^6$ s cm^{-2} only (the upper limit of the b values normally used in diffusion weighted MRI), one can see that only monoexponential decay is observed. The ADC obtained is insensitive to the diffusion time and is about $0.26(\pm 0.02) \times 10^{-5}$ cm^{2}s^{-1}. This value is well within the range previously reported for water in ischemic brain tissue (*3–10*). Our value is more toward the lower end of the reported range but it should be noted that our measurements were performed at 25°C, a temperature which is lower than the *in vivo* cases studied previously.

Comparing the bi- and triexponential fits of the experimental data (Table 1, Figs. 2A and 2B) raises an additional interesting point. Up to b values of $1–2 \times 10^6$ s cm^{-2} both the bi- and triexponential fits seems to be very similar and practically the biexponential fit gives very good agreement with the experimental results. The superiority of the triexponential fit as compared to the biexponential fit is apparent only at b values larger than $2–3 \times 10^6$ s cm^{-2}. Interestingly, Ref. (*47*), in which a clear biexponential decay was observed, was performed using a b value of 1×10^6 s cm^{-2} (see for example Figs. 3a and 3b in Ref. (*47*), in comparison to Fig. 1B). Regarding the fact that we observe a dependency of brain ADCs on the diffusion times, it should be noted that up to b values of 1×10^6 s cm^{-2}, according to our data, there is hardly any difference even when screening a wide range of diffusion times (between 35 and 305 ms). Only at b-values above $2–3 \times 10^6$ s cm^{-2} while covering a large range of diffusion times the effect of t_D is apparent (see Fig. 1 and Table 1). Interestingly, the change in the attenuation $\ln(I/I_0)$ as a function of the diffusion time in our experiments shows the same trend as the theoretical model introduced by Karger *et al.* (*48*) to which accepted physiological values where incorporated (see Fig. 9 in Ref. *47*). However, the experimental results in Ref. *47* failed to reproduce this dependency. In Ref. *47* where diffusion times in the range of 8.4 to 60 ms were used, the authors pointed out that in order to be able to see the effect of the diffusion time better, larger range of diffusion times should be studied as we have done in the current study.

Now that several populations have been identified in the diffusion experiments, it is tempting to try to assign the different populations to physiological populations known to exist in brain tissue. In order to better correlate physiological populations with the apparent populations in the diffusion experiments, it is crucial to study also the relaxation characteristics of the sample. We have found only one T_1 value (2.1 ± 0.1 s) and two T_2 values for the water signal as shown in Table 2. Since only one T_1 value was found and since it is much greater than all the T_M values used in the different diffusion experiments, it seems that the effect of T_1 on the relative populations found in the diffusion experiments acquired at different T_M is insignificant. So the change in the relative population found in the diffusion experiments cannot be attributed to the different T_1 of the different water populations.

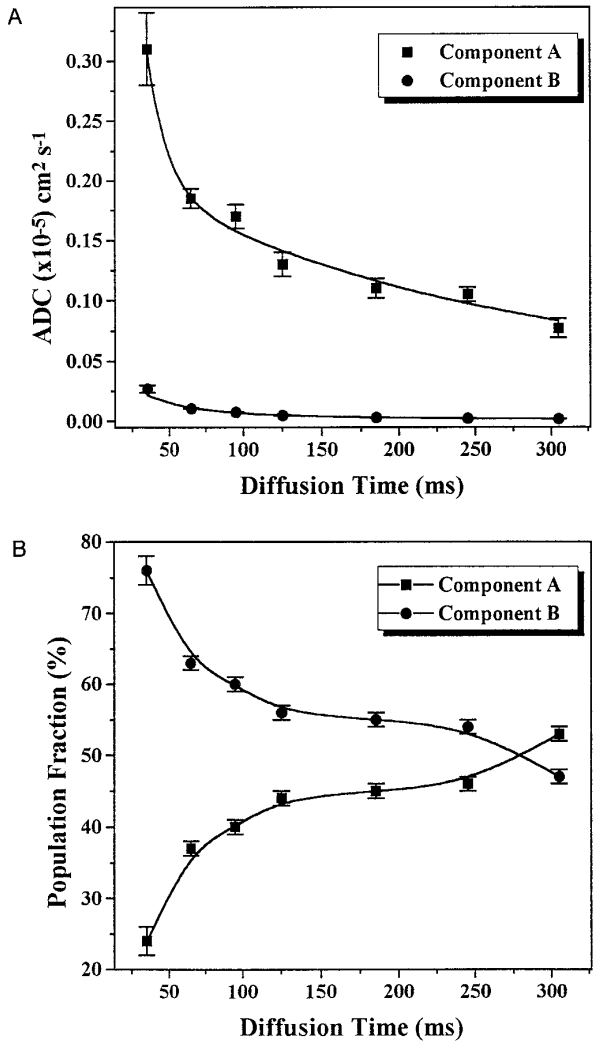

FIG. 9. The effect of the diffusion time ($\Delta - \delta/3$) on the (A) ADCs and (B) relative populations of NAA ($n = 3$) as obtained from the biexponential fit. It is clear that both ADCs decrease with the increase in t_D and their relative populations nearly equalize at long diffusion times. The solid lines are arbitrary and are used just to guide the eye.

The CPMG experiments revealed two different T_2 values. The minimal TE used in the current diffusion experiments is 70 ms, which is longer than five times the T_2 of the fast relaxing component. Therefore, this component should have an insignificant effect on the signal in our diffusion experiments. Therefore, in practice, the signal which contributes to our diffusion experiments has only one T_2. If this is correct one should expect, the TE to have no effect on the diffusion results, in the absence of background gradients. The results of diffusion experiments in which only the TE has been changed are depicted in Table 3. As expected, the change in the TE had no effect on the relative populations as deduced from the diffusion experiments.

Assignment of the two diffusion components found in brain tissue to the two major physiological compartments, namely the intracellular and the extracellular spaces, seems plausible at first glance. In the case of the biexponential fit we found that the population ratio is around 4, which is in good agreement with the relative populations of these two physiological compartments. However, it should be noted that the component whose fraction amounts to 80% of the total population and thus should be assigned to the intracellular space is the one that has the high ADC. As it is agreed that the ADC of the intracellular water is much lower than that of the water in the extracellular space, such an assignment seems problematic. It is interesting to note that in the other study in which biexponential decay was observed (*47*), there was also no agreement between the relative populations found in the diffusion experiments and the relative sizes of the intra- and extracellular spaces. One plausible explanation for the fact that the sizes of the compartments extracted from the diffusion experiments do not match the sizes of known physiological compartments may be exchange between those compartments which is not taken into account by Eq. [2].

An additional important result is that with the change in t_D one observes changes in the relative populations of the different diffusing components. Interestingly, at long diffusion times (305 ms) there is, in fact, nearly only a single population. This may imply that at long diffusion times (305 ms) a large fraction of the water molecules have the

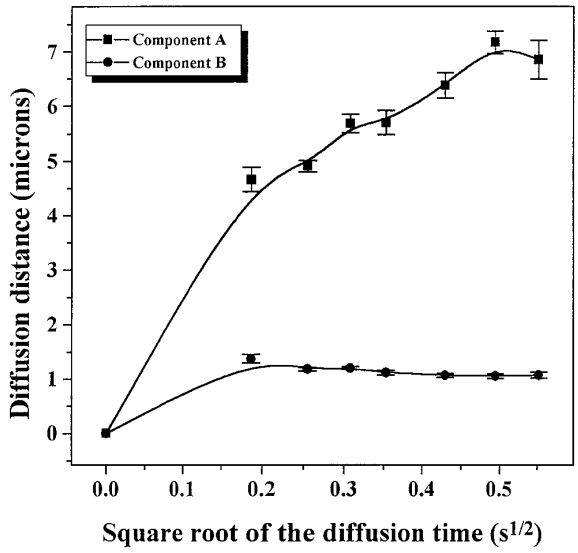

FIG. 10. The ''restriction test'' for the two diffusion components of NAA ($n = 3$). The diffusion distance as a function of the square root of t_D deviates from linearity for both diffusing components. These deviations are much more dramatic than those of brain water and even the fast diffusing component shows a significant restriction. The diffusion paths of the fast and slow diffusing components are around 6–7 and 1–1.5 μm, respectively. The solid lines are arbitrary and are used just to guide the eye.

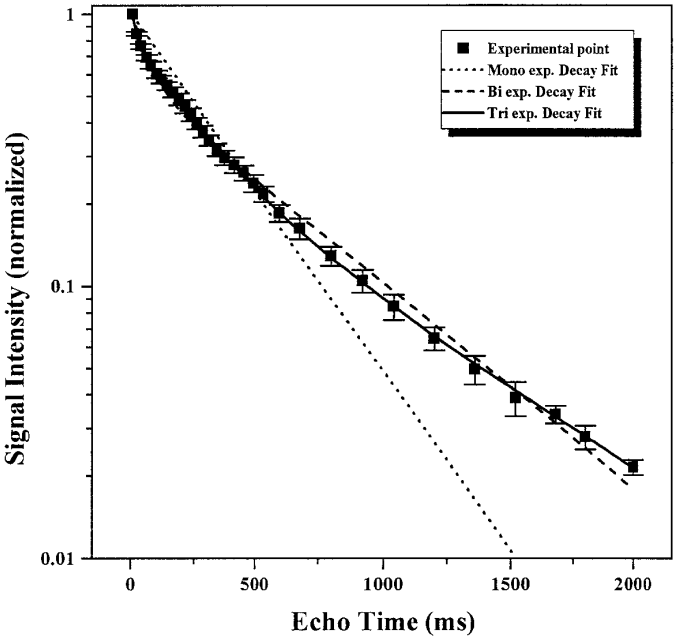

FIG. 11. The T_2 data ($n = 3$) of NAA in excised brain tissue obtained from the CPMG experiment along with the mono-, bi-, and triexponential fitting functions. Very good agreement is obtained between the experimental data and the triexponential fitting function (the numerical results are reported in Table 2).

time to exchange between the compartments, thus canceling the clear distinction between the intra- and extracellular spaces. This is corroborated by a recent study from the Leibfritz group that estimated that the exchange time of water across the membrane is on the order of 25 ms (*50*), meaning that at a diffusion time of 305 ms water molecule exchange between the compartments approaches the fast exchange limit behavior (only one averaged population) (*50*). Therefore, one should refer to apparent populations or apparent fractions when the marker is a molecule that can exchange between compartments. This may also provide a possible explanation for the disagreement between the relative populations found in the diffusion experiments and the real physiological population of each compartment. In addition, it should be noted that the different compartments may be characterized by different T_2 values. If the T_2 of the intracellular space is shorter than that of the extracellular space and since there is a significant T_2-weighting in most diffusion experiments it is possible that some of the disagreements are due to T_2 effect. This is extremely important in the present study as the shortest TE used due to gradient system capability was 70 ms. A better correlation between the populations extracted from the diffusion experiments and known physiological and structural compartments is expected when the diffusion experiments will be acquired using very short diffusion times and very short TE. Since water molecules are present in all the compartments and can exchange among them relatively quickly, rigid delineation and differentiation between the different compartments using diffusion of water molecules is difficult. Therefore, one plausible explanation may be that at t_D of 35 ms we are in the intermediate exchange mode while at t_D of 305 ms we are approaching the fast exchange mode. To verify further the relative importance of exchange, the experimental decay curves were compared to simulated decay curves obtained from the two-sites exchange model of Krager (*48*) as shown in Fig. 12. Interestingly, it has been found that

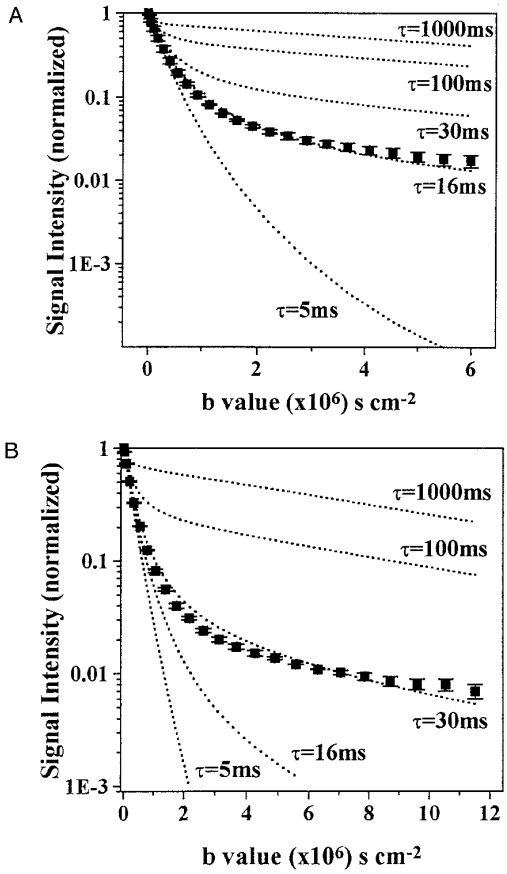

FIG. 12. Comparison between the experimental diffusion decay curves of water in brain tissue ($n = 3$) and the simulated curves obtained from the Krager two sites exchange model for two diffusion times: (A) diffusion time ($\Delta - \delta/3$) of 65 ms and (B) diffusion time of 125 ms. The simulations were performed using the following parameters: $D_A = 2 \times 10^{-5}$ cm^2 s^{-1}, $f_A = 0.2$, $D_B = 0.01 \times 10^{-5}$ cm^2 s^{-1}, $f_B = 0.8$, $\delta = 15$ ms, G variable from 0 to 24 gauss cm^{-1}, $\tau_A = 0.25\tau_B$, and diffusion times of 65 and 125 ms for Figs. 12A and 12B, respectively. The different half life times (τ) used in the simulations are indicated on the specific curves. Figure 12B shows that the data used to simulate the experimental results obtained for diffusion time 65 ms are very different from the experimental results obtained at diffusion time 125 ms. This result suggests that the two sites exchange model cannot account for all the experimental results, implying that some other factors (other than exchange) are also important.

there is no single set of parameters which could fit the entire experimental data. The parameters which seem to fit the experimental curve at t_D of 65 ms (Fig. 12A) are not suitable for fitting the experimental decay curve obtained at t_D of 125 ms (Fig. 12B), indicating that exchange alone cannot totally explain the experimental results. We have found the half-life of water in brain tissue to be on the order of 20 ms, a result which is very similar to that of recent reports by the Leibfritz group (*50*). These simulations clearly indicate that exchange is important but cannot account alone for the entire set of experimental results.

This implies also that most of the water molecules should exhibit little restriction and the plot of the diffusion distance as a function of $\sqrt{t_D}$ should indicate the presence of a semipermeable barrier. This is indeed the case, at least for the large and fast diffusing components, as seen in Figs. 5A and 5B. These graphs show that the fast diffusing components do not reach an asymptotic value and in fact after a minor deviation from linearity, at the longer diffusion times the diffusion distance is a linear function of $\sqrt{t_D}$, implying no restriction. Therefore, it seems that when structural information is requested one should try to monitor the diffusion characteristics of other molecules which have nonuniform distribution among the different compartments and which do not exchange among them. One such obvious candidate for reporting about the intracellular space in brain tissue is NAA.

Diffusion Characteristics of NAA in Brain Tissue

Very few diffusion experiments have been performed on brain metabolites (*36–43*) and the effect of the diffusion time on the diffusion of brain NAA has been reported only for the single exponential decay of NAA (*42, 43*).

The present study show that the signal attenuation of NAA due to diffusion is biexponential and depends heavily on the diffusion time. Additionally the following characteristics have been observed: (1) The ADCs of the NAA decrease considerably with increased of t_D. (2) In the low b value range (up to 0.5×10^6 s cm^{-2}) the decay is monoexponential, but the ADC obtained does decrease with the increase in t_D (Fig. 7B). This observation is in contrast to water diffusion, in which the ADC obtained from the monoexponential fit (in the range of low b values) was insensitive to t_D. (3) The ADC obtained from the range of low b values is in good agreement with those reported in recent publications (*38, 41*). (4) The deviation of the signal attenuation of NAA from linearity shows the opposite trend to that of brain water. In the case of NAA the deviation from linearity increases with the increase in the diffusion time (see Fig. 7A).

One of the surprising results is that we found two different populations of NAA. The larger of these two is the slow component, which has a very low ADC. One possibility that we had to negate was that the signal at 2.023 ppm attributed to NAA contained a contribution from other components such as lipids or other *N*-acetyl groups attached to larger molecules which are characterized by slow diffusion. Since the experiments were performed on a 11.7 T magnet the contribution of *N*-acetyl aspartylglutamate (NAAG) appearing at 2.05 ppm (*34*) could be ruled out as its absorption is well separated from that of NAA and no changes in the chemical shift of the peak were observed when the b value was increased. Additionally, it is well known that NAAG concentration in the rat brain is low and the slow component found in the diffusion experiments amounts to 75% of the total NAA pool (*34*).

In order to verify that the slow diffusing components are not due to larger molecules with the same chemical shift, we measured the ADCs of the two components as a function of TE. Assuming that the slow diffusing component arises from larger molecules, one can expect that this component will be characterized by a short T_2. Accordingly, an increase in the TE should bring about a reduction in the relative population of the slow diffusing component. However, the opposite trend is observed (Table 4) and increasing the TE only brought about an increase in the relative population of the slow diffusing component of the NAA peak. These results suggest that the fast and slow diffusing components of the signal at 2.023 ppm are more likely to represent two different populations of NAA.

NAA is a metabolite known to be present only in the intracellular space of neurons (*51*) and as such one should expect only one diffusing component. However, the results clearly indicate the existence of two diffusing components of nearly the same size. Since NAA is distributed in the intracellular space only, the assignment of each of the diffusing components to physiological populations is not straightforward. In order to do this we first had to measure the T_1 and T_2 relaxation times of the NAA peak in order to estimate their relative effect on our diffusion measurements. This enabled us to estimate the T_1 effects when changing t_D (by changing T_M) and to estimate the visibility of the different populations in our diffusion experiments (see Table 2).

In the T_2 experiments three main populations were identified, as shown in Fig. 11. The one having a T_2 of 19 $\pm$ 3 ms (27 $\pm$ 3%) contributes very little to our diffusion experiments, in which the shortest TE was set to 70 ms. Therefore we are left with the other two T_2 components, namely those having T_2 values of 241 $\pm$ 24 ms (40 $\pm$ 5%) and 686 $\pm$ 56 ms (33 $\pm$ 3%). Since we identified a slow and a fast diffusing component it is tempting to associate them with the fast and slow relaxing components, respectively. A T_2 of a specific population can only be equal to or less than its T_1. The two T_1 values obtained were 410 $\pm$ 10 and 1420 $\pm$ 60 ms. Therefore, the T_1 of the slow diffusing

component which has the longer T_2 (i.e., 686 ± 56 ms) should be the longer one, i.e., 1420 ± 60 ms.

In order to further verify this point and estimate the effect of the T_1 relaxation time on the populations extracted from the diffusion experiments acquired at different t_D, we performed two experiments using the sequence

$$\pi-\tau_0-\pi/2-\tau_1-g-\tau_2-\pi/2-T_M-\pi/2-\tau_2-g-\tau_1-Acq, \quad [II]$$

where τ_0 was set to 300 ms and 1000 ms, which are the null points of the two T_1 values obtained from the inversion recovery experiments. If one ADC is associated with a certain T_1, one should observe a drastic change in the relative population obtained in the diffusion experiments using sequence II when τ_0 is set to $T_1 \cdot \ln 2$ of one component. Interestingly, when τ_0 was set to 1.0 s there was a drastic decrease in the signal-to-noise ratio (SNR); however, the same ADCs were obtained without significant effect on their relative populations. For $\tau_0 = 300$ ms there was only a small decrease in SNR and here again nearly no effect on the relative populations of the two ADCs was observed. This may suggest that both the fast and slow diffusing components have similar T_1 (i.e., 1420 ms), a fact that implies that T_1 effects during the change of T_M from 5 to 275 ms should be minimal.

As stated, the ADCs of both components of the NAA decrease considerably with the increase in t_D. The ADC of the fast component of the NAA decreases by a factor of 6 while the ADC of the slow component decreases by more than an order of magnitude. The deviation from linearity of $\ln(I/I_0)$ as a function of t_D shows a trend opposite to that of brain water but follows the trend reported very recently for water in isolated optic nerve (*32*). Both the slow and fast diffusing components show a marked restriction, as shown in Fig. 10. Interestingly, here it seems that the two barriers have a relatively low permeability and the plateau of the diffusion path suggests the existence of two main compartments, one having a size of about 6–7 μm microns and another on the order of 1 to 2 μm. Based on these observations we tend to speculate that the two populations of NAA are NAA molecules in cell bodies and in fibers (axons), which are known to have a diameter of approximately 1 μm in rat brains (*51–52*). The slow diffusion component, which seems to be restricted in a compartment having a size of around 1 μm, is also characterized by a long T_2 and comprises 75% of the NAA pool (at TE of 70 ms without correction for T_2 relaxation). It has recently been demonstrated that water in the intra-axonal space of sciatic nerve has the longest T_2 as compared to its other compartments (*53*). At first it seems surprising that the slow diffusing component is the larger one; however, it should be noted that the average volume within the axons is comparable to and even larger than that in the cell bodies of the neurons because they are much longer. Therefore it seems plausible to assign the two diffusing components to the two physiological compartments, i.e., NAA molecules in the soma and intra-axonal spaces.

CONCLUSIONS

We have demonstrated that the decay of the signals of water and NAA due to diffusion in brain tissue is not monoexponential but depends on the diffusion time when high *b* values are used. More importantly, we have demonstrated that different results are obtained from the same data set at different ranges of *b* values. In the range of low *b* values ($b \leq 0.5 \times 10^6$ s cm^{-2}), which is the range routinely used in diffusion weighted MRI, a monoexponential decay which is insensitive to the diffusion time is obtained for brain water. For *b* values up to $1-2 \times 10^6$ s cm^{-2} a biexponential decay is observed. Only when larger *b* values are used is the superiority of fitting the experimental data with a triexponential function apparent. In these cases the ADCs obtained do depend on the diffusion times and seem to indicate the presence of restricted diffusion when the major fast diffusing component shows only limited restriction. Therefore it is important to report the entire set of parameters used to obtain the data (such as effective *b* values range, diffusion time, diffusion gradients duration, and TE) when one reports ADC values of brain tissue obtained by NMR measurements. This will allow the results to be put into the context of previous results and increase our ability to reconcile apparent contradictory results. Nevertheless, the assignment of the different diffusing components to known physiological compartments is not straightforward, partially because of exchange.

Surprisingly, NAA signal decay due to diffusion was found to be biexponential and here again it seems that at low *b* values (0.5×10^6 s cm^{-2}) a monoexponential decay is observed as reported recently (*38, 41*). As expected, the ADCs of NAA are much more sensitive to the diffusion time and seem to exhibit restricted diffusion. As such, NAA in our system and under the conditions used seem to have two main compartments, one having a size of 6–7 μm (with fast diffusion and a short T_2) and the other on the order of 1–2 μm (slow diffusion and a long T_2), which may tentatively be assigned to neuronal cell bodies and axons, respectively. Although NAA diffusion is more difficult to obtain it seems to be a better reporter, at least with regard to the neuronal intracellular space, as compared to brain water, which appears in all compartments and exchanges quickly among them. It should be noted that simulations of the NAA diffusion data using the Krager's two sites exchange model (*48*) have shown that even with very long half-life ($\tau \approx$ 1000 ms) there is no agreement between the simulations and

the experimental data. This result indicates that the exchange is much slower than in the case of water and consequently has only a limited effect on the results extracted from NAA diffusion experiments (*54*).

Therefore, we believe that these results show that diffusion characteristics of NAA as a function of t_D have the potential to report the intracellular geometry. *In vitro* NAA diffusion measurements as a function of t_D on excised nerves, which are known to have a much more defined geometry, are under way.

Although the results obtained in this study were obtained for *in vitro* brain tissue their relevance to the *in vivo* state is supported by the similarity of our results to the *in vivo* results reported recently when we analyzed our data using the *b*-value range used in Ref. (*47*). In addition, we have demonstrated that the parameters measured change only very little during the experimental time due to tissue disintegration. Although it is not clear if triexponential decay will be observed *in vivo* it should be noted that a recent *in vivo* ^{2}H DQF study on brain water does corroborate the existence of three water populations (*45, 46*). We agree that *in vitro* experiments should provide a basic platform to give clinically measured ADCs more physical and even physiological meaning (*32*). *In vitro* experiments allow acquisition of a much larger data set with much higher quality, on the basis of which the basic phenomena can be discussed. Based on this knowledge, selected *in vivo* experiments should be performed. Currently we are using NAA diffusion weighted spectroscopy to characterize the intracellular space of neurons *in vivo* both in the normal and in different pathophysiological states.

ACKNOWLEDGMENT

We thank the Ministry of Health of the state of Israel for financial support.

REFERENCES

1. D. Le Bihan, E. Breton, D. Lallemand, P. Grenier, E. Cabanis, and M. Laval-Jeantet, *Radiology* **161,** 401–407 (1986).
2. D. Le Bihan, E. Breton, D. Lallemand, M.-L. Aubin, J. Vignaud, and M. Laval-Jeantet, *Radiology* **168,** 497–505 (1988).
3. D. Le Bihan (Ed.), ''Diffusion and Perfusion Magnetic Resonance Imaging,'' Raven Press, New York (1995), and references cited therein.
4. M. E. Moseley, Y. Cohen, J. Mintorovitch, L. Chileuitt, H. Shimizu, J. Kucharczyk, M. F. Wendland, and P. R. Weinstein, *Magn. Reson. Med.* **14,** 330–346 (1990).
5. M. E. Moseley, J. Kucharczyk, J. Mintorovitch, Y. Cohen, J. Kurhanewicz, N. Derugin, H. Asgari, and D. Norman, *Am. J. Neuroradiol.* **11,** 423–429 (1990).
6. K. Minematsu, L. Li, M. Fisher, C. H. Sotak, M. A. Davis, and M. S. Fiandaca, *Neurology* **42,** 235–240 (1992).
7. S. Warach, D. Chien, W. Li, M. Ronthal, and R. R. Edelman, *Neurology* **42,** 1717–1723 (1992).
8. A. L. Busza, K. L. Allen, M. D. King, N. van Bruggen, S. R. Williams, and D. G. Gadian, *Stroke* **23,** 1602–1612 (1992).
9. T. Back, M. Hoehn-Berlage, K. Kohno, and K.-A. Hossmann, *Stroke* **25,** 494–500 (1994).
10. K.-A. Hossmann and M. Hoehn-Berlage, *Cerebrovasc. Brain Metab. Rev.* **7,** 187–217 (1995).
11. C. C. Hanstock, A. I. Faden, M. R. Bendall, and R. Vink, *Stroke* **25,** 843–848 (1994).
12. J. Ito, A. Marmarou, P. Barzo, P. Fatouros, and F. Corwin, *J. Neurosurg.* **84,** 97–103 (1996).
13. Y. Assaf, E. Beit-Yannai, E. Shohami, E. Berman, and Y. Cohen, *Magn. Reson. Imaging* **15,** 77–85, 1997.
14. M. Eis, T. Els, and M. Hoehn-Berlage, *Magn. Reson. Med.* **34,** 835–844 (1995).
15. L. L. Latour, Y. Hasegawa, J. E. Formato, M. Fisher, and C. H. Sotak, *Magn. Reson. Med.* **32,** 189–198 (1994).
16. H. Benveniste, L. W. Hedlund, and G. A. Johnson, *Stroke* **23,** 746–754 (1992).
17. Y. Hasegawa, L. L. Latour, C. H. Sotak, B. J. Dardzinski, and M. Fisher, *J. Cereb. Blood Flow Metab.* **14,** 383–390 (1994).
18. J. A. Helpern, R. J. Ordidge, and R. A. Knight, *in* ''11th Annual Meeting of the Society of Magnetic Resonance in Medicine,'' p. 1201 (1992). [Abstract]
19. H. B. Verheul, R. Balazs, J. W. Berkelbach van der Sprenkel, C. A. F. Tulleken, K. Nicolay, K. S. Tamminga, and M. van Lookeren Campagne, *NMR Biomed.* **7,** 96–100 (1994).
20. A. van der Toorn, E. Sykova, R. M. Dijkhuizen, I. Vorisek, L. Vargova, E. Skobisova, M. van Lookeren Campagne, T. Reese, and K. Nicolay, *Magn. Reson. Med.* **36,** 52–60 (1996).
21. D. G. Norris, T. Niendorf, M. Hoehn-Berlage, K. Kohno, E. J. Schneider, P. Hainz, M. Hropot, and D. Leibfritz, *Magn. Reson. Imaging* **12,** 1175–1182 (1994).
22. D. G. Norris, T. Niendorf, and D. Leibfritz, *NMR Biomed.* **7,** 304–310 (1994).
23. C. Beaulieu and P. S. Allen, *Magn. Reson. Med.* **31,** 394–400 (1994).
24. C. Beaulieu, M. D. Does, R. E. Snyder, and P. S. Allen, *Magn. Reson. Med.* **36,** 627–631 (1996).
25. A. Szafer, J. Zhong, and J. C. Gore, *Magn. Reson. Med.* **33,** 697–712 (1995).
26. A. W. Anderson, J. Zhong, O. A. C. Petroff, A. Szafer, B. R. Ransom, J. W. Prichard, and J. C. Gore, *Magn. Reson. Med.* **35,** 162–167 (1996).
27. L. L. Latour, K. Svoboda, P. P. Mitra, and C. H. Sotak, *Proc. Natl. Acad. Sci. U.S.* **91,** 1229–1233 (1994).
28. D. Le Bihan, *NMR Biomed.* **8,** 375–386 (1995).
29. J. E. Tanner, *J. Chem. Phys.* **52,** 2523–2526 (1970).
30. P. van Gelderen, M. H. M. de Vleeschouwer, D. DesPres, J. Pekar, P. C. M. van Zijl, and C. T. W. Moonen, *Magn. Reson. Med.* **31,** 154–163, 1994.
31. T. Niendorf, D. G. Norris, and D. Leibfritz, *Magn. Reson. Med.* **32,** 672–677 (1994).
32. G. J. Stanisz, A. Szafer, G. A. Wright, and R. M. Henkelman, *Magn. Reson. Med.* **37,** 103–111 (1997).
33. D. L. Birken, and W. H. Oldendorf, *Neurosci. & Biobehavioral Rev.* **13,** 23–32 (1989).
34. J. Frahm, T. Michaelis, K.-D. Merboldt, W. Hanicke, M. L. Gyngell, and H. Bruhn, *NMR Biomed.* **4,** 201–204 (1991).

35. C. T. W. Moonen, P. C. M. van Zijl, D. Le Bihan, and D. DesPres, *Magn. Reson. Med.* **13,** 467–477 (1990).

36. S. Posse, C. Decarli, and D. Le Bihan, *Radiology* **188,** 719–725 (1993).

37. S. Posse, C.-A. Cuenod, and D. Le Bihan, *in* ''Diffusion and Perfusion Magnetic Resonance Imaging'' (D. Le Bihan, Ed.), pp. 57–62, Raven Press, New York (1995).

38. K. Nicolay, A. van der Toorn, and R. M. Dijkhuizen, *NMR in Biomed.* **8,** 365–374 (1995).

39. K.-D. Merboldt, D. Horstermann, W. Hanicke, H. Bruhn, and J. Frahm, *Magn. Reson. Med.* **29,** 125–129 (1993).

40. M. Wick, Y. Nagatomo, F. Prielmeier, and J. Frahm, *Stroke* **26,** 1930–1934 (1995).

41. A. van der Toorn, R. M. Dijkhuizen, C. A. F. Tulleken, and K. Nicolay, *Magn. Reson. Med.* **36,** 914–922 (1996).

42. C. T. W. Moonen, P. van Gelderen, P. C. M. van Zijl, D. DesPres, and A. Olson, *in* ''Tenth Annual Meeting of the Society of Magnetic Resonance in Medicine,'' p. 141 (1991). [Abstract]

43. P. C. M. Van Zijl, D. Davis, and C. T. W. Moonen, *in* ''NMR in Physiology and Biomedicine'' (R. J. Gillies, Ed.), pp. 185–198, Academic Press, San Diego (1994).

44. E. Von Meerwall and M. Kamat, *J. Magn. Reson.* **83,** 308–323 (1989).

45. Y. Assaf and Y. Cohen, *J. Magn. Reson. B* **112,** 151–159 (1996).

46. Y. Assaf, G. Navon, and Y. Cohen, *Magn. Reson. Med.* **37,** 197–203 (1997).

47. T. Niendorf, R. M. Dijkhuizen, D. G. Norris, M. van Lookeren Campagne, and K. Nicolay, *Magn. Reson. Med.* **36,** 847–857 (1996).

48. J. Karger, H. Pfeifer, and W. Heink, *Adv. Magn. Reson.* **12,** 1–89 (1988).

49. J. Pfeuffer, U. Flogel, N. Serkova, W. Dreher, and D. Leibfritz, *in* ''Proceedings of the Fourth Meeting of the International Society for Magnetic Resonance in Medicine,'' p. 261 (1996). [Abstract]

50. J. Pfeuffer, C. Meier, W. Dreher, and D. Leibfritz, *in* ''Proceedings of the Fifth Meeting of the International Society for Magnetic Resonance in Medicine,'' p. 1695 (1997). [Abstract]

51. P. Morell, R. H. Quarles, and W. T. Norton, *in* ''Basic Neurochemistry'' (G. J. Siegel, B. W. Agranoff, R. W. Albers, and P. B. Molinoff, Eds.), 5th ed., p. 124, Raven Press, New York (1993).

52. L. P. H. Leenen, J. Meek, P. R. Posthuma, and R. Nieuwenhuys, *Brain Res.* **359,** 65–80 (1985).

53. Y. Seo, H. Shinar, and G. Navon, *in* ''Fourth Annual Meeting of the International Society of Magnetic Resonance in Medicine,'' p. 258 (1996). [Abstract]

54. Y. Assaf and Y. Cohen, *NMR Biomed.,* in press.